Ab Initio Study of the Adducts of Small Molecules with the Isolated Hydroxyl of Silica and the Brønsted Site in Zeolites: A Comparison between B3-LYP and MP2 Methods

B. Civalleri, E. Garrone, and P. Ugliengo*

Dipartimento di Chimica Inorganica, Chimica Fisica e Chimica dei Materiali, Universitá di Torino, Via P. Giuria 7, 10125 Torino, Italy

Received: July 14, 1997; In Final Form: November 17, 1997

A set of adducts of H_3SiOH (SIL) and $H_3Si(OH)AlH_3$ (BRO), minimal cluster models for the isolated hydroxyl species in silica and the Brønsted site in zeolites, respectively, have been studied by the B3-LYP method using various basis sets, including aug-cc-pVDZ and aug-cc-pVTZ. Molecules considered were H_2 (in two configurations), CO, H_2O, and NH_3 with SIL and CO only with BRO: results were compared with similar calculations run at MP2 as well as with experimental results for amorphous silica and proton exchanged zeolites. B3-LYP results were as good as MP2, though a larger basis set dependence is seen for the former. As the interactions studied span a sizable range of energy, a number of correlations are drawn, similar to those usually drawn for experimental data. The case of SIL/NH_3, treated including anharmonicity of the OH motion, shows that SIL is definitively less acidic than the isolated hydroxyl of silica.

1. Introduction

A reliable measure of the acidity of hydroxyls on surfaces or in zeolites is the shift in frequency of the O−H stretching mode caused by the interaction with suitable molecules.[1] This may then be related to other observables, such as the proton affinity of the molecule, the deprotonation energy of the hydroxyl species, etc., in agreement with the general knowledge on H-bonding.[2] For these reasons, several authors have studied the interaction of small molecules with acidic sites in catalysts mainly by means of IR spectroscopy.

On the computational side, the interaction between a base molecule and a surface acidic hydroxyl is usually treated by adopting a cluster approach in the description of the acidic center,[1] whereby the cluster is terminated by hydrogen atoms. The acidic centers most commonly investigated are the isolated hydroxyl at the surface of amorphous silica and the Brønsted acid site in zeolites, referred to hereafter as SiOH and Si(OH)-Al, respectively. Various cluster sizes may be chosen for both, but the minimal ones are at the moment still mandatory when a high-level treatment is requested, including for example the study of the anharmonicity in the O−H motion. Minimal-size clusters correspond to the two molecules H_3SiOH and H_3Si-$(OH)AlH_3$, which are not chemically stable as such: the former rapidly condenses to siloxane and may only be studied as a vanishing intermediate, while the latter is unknown. The two molecules are described in detail below and are referred to in the following as SIL and BRO, respectively.

Previous computational work has concerned, on one hand, SIL alone[3] and in interaction with ammonia,[4] water,[5] formaldehyde,[6] hydrogen,[7,8] carbon monoxide[9−12] and N_2O.[13] As far as BRO is concerned, computational results concern the cluster molecule alone[14] and the interaction with CO,[11,12] C_2H_2, C_2H_4, $CH_3-CC-CH_3$, and CH_3-CC-H.[15]

All these calculations have been run at the SCF level (self-consistent field) or at the MP2 level (perturbative Møller−Plesset method truncated at the second term[16]), that is, with no allowance for electron correlation in the former case and with partial allowance in the latter. An overall agreement between experimental data and computational results has been found. However, computational results show a systematic underevaluation of both heats of adsorption and OH frequency shift as caused by the adsorption process when compared with the corresponding measured quantities. This may be due to an intrinsically weaker acidity of the cluster model with respect to the acidic centers at the surface, both with SIL and BRO, but it could also be related to the computational approaches adopted. To check such a possibility, in the present work we resort to the newly developed, highly fashionable density functional (DF) techniques,[17] which account for electron correlation by means of an a priori well-defined exchange correlation functional. The ability of DF techniques, and in particular of the functional adopted in the present work, referred to hereafter as B3-LYP (see methods section), to deal with weak and medium-strength H-bonds has been proved recently.[18,19]

The systems investigated are SIL alone and in interaction with ammonia, water, carbon monoxide, and hydrogen and BRO alone and in interaction with CO. All such systems have been chosen because their experimental counterparts have been characterized to some extent. As these cases span a sizable range of interaction energies, a few correlations among observables may be drawn. The case of weakest interaction (SIL/H_2) is crucial because previous HF and MP2 calculations yielded conflicting results as to the assumed configuration.

2. Methods

All the calculations have been performed at ab initio level, using the program GAUSSIAN-94:[20] the option for the integration grid for the density functional calculations was set to FINE. The DF method adopted is the one proposed by Becke,[21] based on a three-parameter formula as far as the exchange part is concerned, to include some Hartree−Fock exchange, and on the functional proposed by Yang, Lee, and Parr[22] for correlation. The corresponding MP2 computations have also been carried out, when not already available. Basis sets adopted are Dunning's double-ζ plus polarization functions hereafter referred to as DZP;[23] standard Pople 6-31G(d,p) augmented with a set

S1089-5647(97)02281-5 CCC: $15.00
Published on Web 03/11/1998

of diffuse functions on O, N, Si, and C respectively;[24] the newly developed correlation-consistent basis sets aug-cc-pVDZ and aug-cc-pVTZ.[25]

Geometry optimization has been carried out at all levels of computation, using analytical gradient techniques. Basis set superposition error (BSSE) has been evaluated using the full counterpoise method[26] for all structures.

The binding energy BE of any adduct has been evaluated by subtracting the total energy of the hydroxyl species and the base molecule from that of the adduct itself calculated at the same level of treatment.

Harmonic normal-mode frequencies have been computed adopting analytical second energy derivatives and solving the equations of nuclear motion by standard methods.[27] Being concerned with frequency shifts rather than absolute values, no empirical scaling of computed harmonic frequencies has been applied.

For the cases of SIL and SIL/NH_3 only, anharmonic O−H frequencies have been obtained under the assumption of the O−H motion as a normal mode.[11] The total energy of the adduct has been computed as a function of the O−H distance, all other geometrical features have been kept constant, and the nuclear Schrödinger equation has been solved numerically by means of a homemade code.[28]

3. Results and Discussion

3.1. The Isolated Hydroxylic Species. The most relevant results for SIL (see Figure 1) together with the experimental results for SiOH are reported in Table 1 and, vide infra, Table 8, respectively.

Changes in geometrical features caused by varying the level of treatment are small. The Si−O bond lengths computed with aug-cc-pVDZ basis set are however systematically longer than the values computed with any other combination of basis set and method, while the Si−O−H angle is systematically smaller. Both features seem to depart from the most accurate CPF values: further work is needed to establish under what conditions convergence is achieved. The deprotonation energy tends to decrease with larger basis sets: values coming from different methods are in fair agreement, as are the experimental value and the most sophisticated computational one, coming from the CPF treatment.[3] It is worth noting that the estimated experimental deprotonation energy of the isolated silanol belonging to the amorphous silica surface is smaller than the value calculated for SIL showing a higher acidity of the former with respect to SIL. The agreement with values computed with other techniques is rather satisfactory, particularly that between the ω_h(OH) values computed at MP2/aug-cc-pVDZ, B3-LYP/aug-cc-pVDZ and MP2/TZ(O)DZP, respectively.

As to the specific intensity of the O−H stretching mode it is observed that B3-LYP yields values somewhat smaller than MP2; the spread in the computed values is however rather limited. The experimental value reported for SiOH is also definitely smaller than the values calculated for SIL.

Table 2 gathers the computational findings for BRO, the geometry of which is depicted in Figure 2. The structure is almost planar, and indeed, the difference in energy between a free C_1 symmetry and a constrained C_s configuration is only 0.073 kJ mol^{-1} at B3-LYP/aug-cc-pVDZ level of treatment. Any experimental data concerning the unknown BRO molecule is obviously lacking. Reference values concern the Si(OH)Al zeolitic species. The harmonic frequency (together with the anharmonicity parameter) has been evaluated by Kazansky and co-workers[31] by measuring a set of overtones: the agreement between calculated and experimental values is satisfactory. The experimental absolute intensity of the OH mode is not available, but an estimate based on the vibrational frequency has been given:[35] as for the SIL case, calculated values for the specific intensity are several times larger than that for Si(OH)Al. There is evidence from previous computational work on small and medium-sized molecules[32] that both MP2 and B3-LYP methods give infrared intensities in reasonable agreement with the corresponding experimental data in gas phase. In contrast, the present computed results for SIL and BRO models are systematically larger than any experimental value for silica and zeolites. This fact, is probably due to the presence, in the real systems, of the surrounding solid, the polarizability of which decreases the flux of charges caused by the OH vibration.

The deprotonation energy has been evaluated both on the basis of IR results[33] and by means of ^{1}H-MAS NMR.[36] The two methods yield comparable results. As to the deprotonation

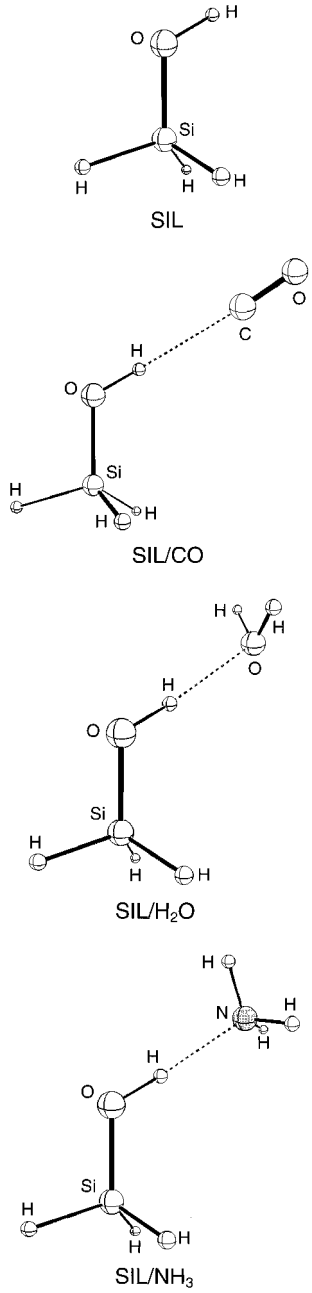

Figure 1. Molecular drawings for SIL and selected adducts. Most relevant geometrical data are reported in Tables 1 and 3−5. (a) SIL and SIL/CO. (b) SIL/H_2O, SIL/NH_3.

TABLE 1: Molecular Properties of SIL by Different Methods[a]

	ΔE_{DP}	ω_h(OH)	I(OH)	O−H	Si−O	∠SiOH
present work						
B3-LYP/DZP	1560	3919	75	0.964	1.661	119.0
B3-LYP/6-31+G(d,p)	1522	3903	87	0.963	1.673	119.2
B3-LYP/aug-cc-pVDZ	1525	3867	76	0.963	1.700	116.5
B3-LYP/aug-cc-pVTZ[h]	1522					
MP2/DZP	1558	3983	91	0.963	1.665	118.8
MP2/6-31+G(d,p)	1524	3953	95	0.962	1.678	118.7
MP2/aug-cc-pVDZ	1516	3870	82	0.965	1.709	115.6
MP2/aug-cc-pVTZ[h]	1514					
previous work						
SCF/TZ(O)DZP[b]	1576	4176		0.946	1.65	120.5
MP2/TZ(O)DZP[b]	1550	3870		0.966	1.67	116.9
CPF/[8s,5p,3d,1f/4s,2p][b]	1531			0.958	1.65	117.7
MP2/cc-pVQZ(-g)[c]	1526			0.955	1.656	117.9
MP4/cc-pVTZ[c]	1541			0.960	1.663	115.7
experimental	1502 ± 21[d]					
	1390 ± 25[e]	3922[f]				
		3941[g]	17[g]			

[a] Energy of deprotonation, ΔE_{DP} (kJ/mol); unscaled harmonic vibrational frequency, ω_h(OH) (cm^{-1}); and infrared intensity, I(OH) (km/mol), of the OH stretching mode and selected bond lengths and angles (angstroms, degrees). [b] Reference 3. [c] Reference 29. [d] Measured for H_3SiOH at room temperature in a tandem flowing afterglow-selected ion flow tube. Reference 30. [e] Silanol groups on silica surfaces. Reference 33. [f] Reference 31. [g] From IR data on aerosil Degussa outgassed at 800 °C. Reference 11. [h] Geometries optimized at aug-cc-pVDZ.

TABLE 2: Molecular Properties of BRO by Different Methods[l]

	ΔE_{DP}	ω_h(OH)	I(OH)	O−H	Si−O	Al−O	∠SiOAl	Al···H(O)
present work								
SCF/DZP		4172		0.947	1.697	2.030	126.2	
B3-LYP/DZP	*m*	3869	138	0.967	1.717	2.023	123.3	2.629
B3-LYP/6-31+G(d,p)	*m*	3862	138	0.966	1.726	2.032	122.2	2.655
B3-LYP/aug-cc-pVDZ	1321	3849	118	0.964	1.749	2.044	121.1	2.676
B3-LYP/aug-cc-pVTZ[n]	1308							
MP2/DZP		3927	160	0.967	1.720	2.030	123.3	
MP2/6-31+G(d,p)	1318	3903[o]		0.966	1.731	2.032	122.9	2.642
MP2/aug-cc-pVDZ[p]	1316							
previous work								
SCF/6-31G(d)[a]	1329	4090		0.951	1.71	2.03	131	
MP2/DZ+2P[b]	1306			0.964	1.67	2.02	130	
MP2/6-31G(d)[a]	1312			0.972	1.72	2.01	124.4	
MP2/6-311G(d,p)[a]	1329							
MP2/6-311+G(3df,2p)[a]	1292							
QCISD(T)/6-311G(d,p)[a]	1338							
G2(MP2)[a]	1301							
experimental	1220 ± 40[c]	3798[i]	32[j]					2.38[k]
	1200[d]							2.48[k]
	1140[e]							
	1170[f]							
	1190[g]							
	1180/1333[h]							

[a] Geometries optimized at MP2/6-31G(d) level. Reference 34. [b] Reference 1. [c] ^{1}H-MAS-NMR spectroscopy in H-ZSM-5 at room temperature. Reference 36. [d] IR data on HNaY, reference 33. [e] IR data on H-MORD, reference 40. [f] IR data on H-ZSM-5, reference 40. [g] IR data on HY, reference 40. [h] IR data on HNa-ZSM-5, references 41 and 42. [i] Bridging hydroxyls. Reference 11. [j] IR data on HY with a ratio Si/Al=2.7. Reference 35. [k] ^{1}H-NMR measurements on HY and H-ZSM-5, respectively. Reference 37. [l] Energy of deprotonation, ΔE_{DP} (kJ/mol); unscaled harmonic vibrational frequency, ω_h(OH) (cm^{-1}); and infrared intensity, I(OH) (km/mol), of the OH stretching mode and selected bond lengths and angles (angstroms, degrees). C_s symmetry imposed. [m] Rupture of the $H_3SiOAlH_3^-$ structure. [n] Geometries optimized at aug-cc-pVDZ. [o] Numerical differentiation. [p] Geometries optimized at 6-31+G(d,p).

energy, B3-LYP with either DZP or 6-31+G(d,p) yields rupture of the $H_3SiOAlH_3$ structure. All other treatments yield values in the range 1290−1340 kJ mol^{-1} (i.e., definitely larger than the experimental estimate of 1220 kJ mol^{-1}): this is probably again indication that also the BRO model is less acidic than the actual acidic center in zeolites.

NMR has also been used to determine the Al···H(O) distance in some zeolitic sites.[37] The values calculated for the Al···H(O) distance are around 2.65 Å, whereas the experimental values in zeolitic systems are definitely smaller (see Table 2): it is unlikely that either better basis set or method will improve the results significantly. Most likely, the absence of proper framework constraints in BRO produces a too narrow Al−O−Si angle as well as a too long Al−O bond length, which, in turn, impart too small of an acidic character to BRO when compared to zeolites.

3.2. Geometry, Binding Energy, and Vibrational Features of the Adducts. All results from our calculations are reported in Tables 3−7, which refer to SIL/NH_3, SIL/H_2O, SIL/CO, BRO/CO, and SIL/H_2, respectively. Equilibrium geometries are described in Figures 1−3. Except for the case of SIL/H_2, which is dealt with separately, the tables report for the three basis sets adopted: (i) a geometric feature, the distance from the acidic proton and the proton-acceptor atom in the molecule, of which in one case (BRO/CO) a direct experimental estimate is reported; (ii) vibrational features (i.e., the shift in frequency and the

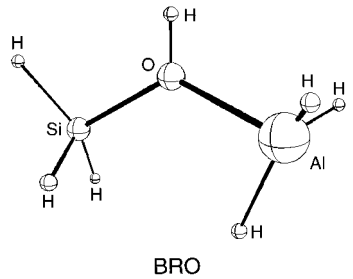

BRO

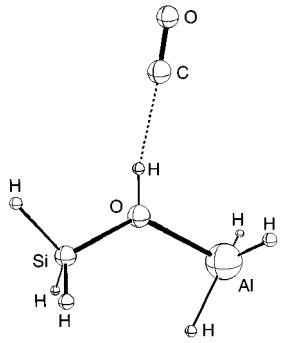

BRO/CO

Figure 2. Molecular drawings for BRO and BRO/CO adducts. Most relevant geometrical data are reported in Tables 2 and 6.

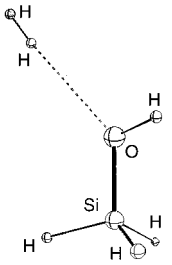

SIL/H_2 (F)

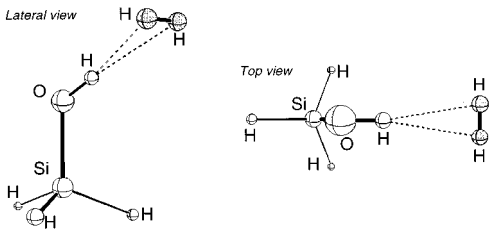

SIL/H_2 (T)

Figure 3. Molecular drawings for F-shaped and T-shaped structures of SIL/H_2 adducts. Most relevant geometrical data are reported in Table 7.

intensity of the O−H stretching mode, the former with respect to the corresponding unperturbed molecule): with CO as a base molecule, the changes in frequency of the C−O stretching mode are also reported; (iii) energetic features, like the binding energy BE, the BSSE, correction and the enthalpy of reaction at absolute zero, obtained from the BSSE-corrected BE by subtraction of the zero-point energy. Also reported in the tables are the available experimental measurements or estimates concerning either SiOH or Si(OH)Al. Anharmonic vibrational data for SIL/NH_3 concerning the computed O−H stretch are reported in Table 8.

3.3. Effect of Basis Set. Inspection of Tables 3−6 shows that the computational findings definitely depend on the adopted basis set, both with MP2 and B3-LYP treatments. The three main observables in the present cases of H-bonding are the enthalpy of interaction at absolute zero $\Delta H°(0)$, the shift $\Delta\omega_h$-(OH) of the stretching mode of the hydroxyl, and the corresponding relative change in intensity, $\Delta I(\mathrm{OH}) = (I_c - I_0)/I_0$. The changes of these three observables as a function of both the type of treatment and the adopted basis set are illustrated in Figure 4 for all cases, except for SIL/H_2, dealt with below. The interaction enthalpy (Figure 4a) for both B3-LYP and MP2 shows an overall decrease in the series DZP, 6-31+G(d,p), aug-cc-pVDZ, except for the SIL/CO case, where it is basically constant. The single-point calculation with aug-cc-pVTZ yields, in contrast, higher values in all cases. A similar behavior is shown by the shifts in the OH frequency (Figure 4b), where, however, single-point data at the aug-cc-pVTZ are obviously lacking. Such features are clearly related to the behavior of the intermolecular distance, which increases with both methods with increasing quality of the basis set (see the tables). Those obtained with B3-LYP are systematically larger: at least for the two more energetic interactions (SIL/H_2O and SIL/NH_3), convergence between the two methods seems to be reached. The intermolecular distance H···C calculated for BRO/CO is in remarkable agreement with the experimental estimate.[38]

Concerning the $\Delta H°(0)$, one may note that the increase brought about by the use of aug-cc-pVTZ basis set is larger for MP2 than for B3-LYP. Since the intermolecular distances calculated at the two levels are rather close, such a discrepancy could be due to the fact that MP2, in contrast with DFT, is able to take into account to some extent the dispersive interaction between the two moieties of the adducts. Also worth noting is the reduced BSSE in the B3-LYP case when compared to MP2 results.

The computed values of $\Delta\omega_h(\mathrm{OH})$ are systematically larger with B3-LYP than with MP2. Again, convergence seems to be reached at least for the two more energetic interactions. We have recently shown[19] for the case of fluoridic acid adducts that all DFT methods tend to overestimate the ω(FH) shift because of the incomplete cancellation of the spurious self-interaction contribution, particularly severe for the hydrogen atom. Among DFT methods, however, B3-LYP is the one which suffers less self-interaction due to favorable Hartree−Fock exchange in the definition of the exchange functional. For both SIL/CO and BRO/CO adducts, the blue-shift suffered by the ω_h(CO) stretching frequency has been computed. Comparison with the available experimental measurements reveals that (i) the basis set dependence of the $\Delta\omega_h$(CO) value is larger for B3-LYP than that for MP2 data, (ii) too small basis sets tend to overestimate the absolute shift with respect to experimental measurements as it is clearly shown for the BRO/CO adduct (see Table 6). Our best estimates (i.e., B3-LYP/aug-cc-pVDZ or MP2/aug-cc-pVDZ) are in excellent agreement with the data obtained on amorphous silica and in a number of acidic zeolites.

Inspection of Tables 1 and 2 shows that the basis set dependence of the unscaled harmonic ω_h(OH) frequency for both SIL and BRO models is larger for MP2 than for B3-LYP method. Quite surprisingly, the basis set dependence of the $\Delta\omega_h$(OH) is far larger for the B3-LYP method than that for the MP2 technique: in that respect, vibrational shifts computed with DF methods adopting too small basis sets (for instance the widespread 6-31G(d,p)) are to be taken with some caution. We do not have a straightforward explanation for that: one possibility is that the self-interaction error becomes more relevant for the case of interacting molecules, because of the hydrogen bond interaction.

As to the infrared intensities (Figure 4c), they appear basically insensitive to the basis set, whereas one method (MP2) yields systematically lower values than the other.

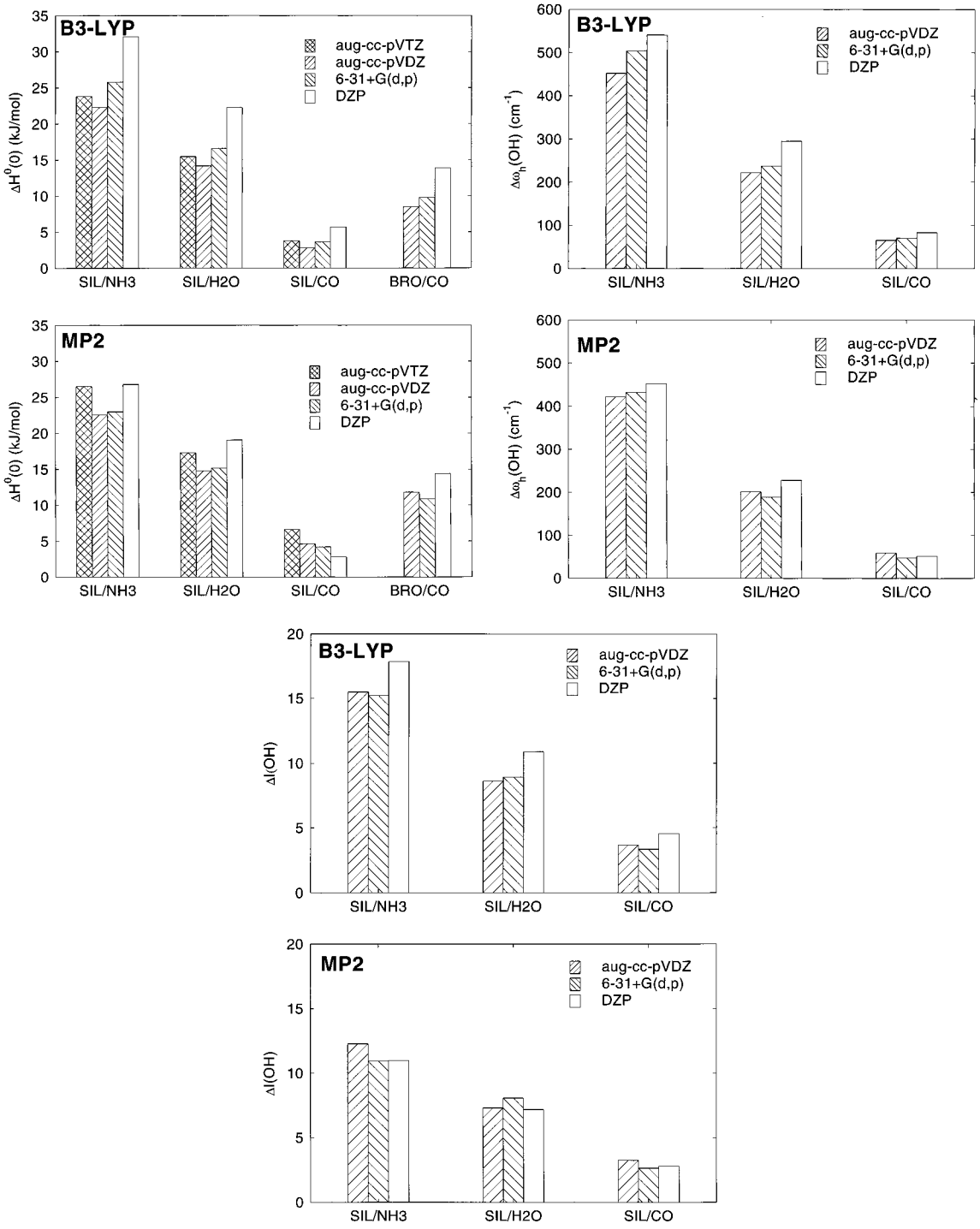

Figure 4. Method and basis set dependencies for computed (a) $\Delta H°(0)$ (kJ/mol), (b) $\Delta\omega_h$(OH) (cm^{-1}), and (c) $\Delta I(\mathrm{OH}) = (I_c - I_0)/I_0$.

3.4. Adduct SIL/H_2. As already stated, previous calculations run at SCF level[7,8] showed that the two configurations in Figure 3, in which dihydrogen is acting either as H-acceptor (T-shaped structure) or H-donor (F-shaped structure), had nearly the same energy. MP2 calculations were in slight favor of the T-structure.

Table 7 compares the results obtained in the present work using the aug-cc-pVDZ and aug-cc-pVTZ basis sets with experimental data and literature computational results. Even our best calculations yield unbound adducts, after correction for BSSE and ZPE, in agreement with what was already found. If reference is made to BE values corrected only for BSSE (hereafter referred to as BE(CPC)), it is found that, accordingly to our best calculations, the T-shaped configuration is in all cases slightly more stable than the F-shaped. This is illustrated in Figure 5, which also reports the results of lower-level calculations, favoring instead the F-shaped structure.

The MP2 $\Delta\omega$(HH) computed for the T-shaped adduct is two times larger than the corresponding B3-LYP value: an opposite behavior, however, is seen for $\Delta\omega_h$(OH), which B3-LYP value is grossly overestimated when compared to the experiment.

3.5. Correlations between Different Observables. It is well-known in the literature of H-bonding that some of the observables dealt with in the present paper are related to each other (e.g., the binding energy BE, the shift $\Delta\omega_h$(OH), and the intensity shift of the same mode). In the following, correlations between such quantities are considered, concerning the three basis set adopted, and both MP2 and B3-LYP methods.

TABLE 3: SIL/NH_3 System[a]

present work	BE (BSSE)	$\Delta H°(0)$	ΔI(OH)	$\Delta\omega_h$(OH)	r(H···N)
B3-LYP/DZP	−45.9 (4.4)	−32.1	18	−541	1.806
B3-LYP/6-31+G(d,p)	−40.1 (4.9)	−25.8	15	−504	1.843
B3-LYP/aug-cc-pVDZ	−33.1 (2.5)	−22.3	16	−452	1.872
B3-LYP/aug-cc-pVTZ[b]	−32.6 (0.5)	−23.8			
MP2/DZP	−45.1 (8.9)	−26.8	11	−452	1.845
MP2/6-31+G(d,p)	−41.9 (10.0)	−23.0	11	−432	1.867
MP2/aug-cc-pVDZ	−37.0 (6.3)	−22.6	12	−422	1.871
MP2/aug-cc-pVTZ[b]	−37.4 (2.8)	−26.5			
previous work					
SCF/DZP[c]	−32.5 (2.4)			−279	2.000
SCF/TZ+(2d,2p)[c]	−25.9				
MP2/TZ+(2d,2p)[c]	−36.5				
experimental		−37[d]		−950[f]	
		−15/−60[e]			

[a] Interaction energies, BE (kJ/mol); basis set superposition error BSSE (kJ/mol), heat of formation $\Delta H°(0)$ at 0 K corrected for BSSE; relative change in infrared intensity of the harmonic O−H stretching mode, $\Delta I(\mathrm{OH})=(I_c - I_0)/I_0$; harmonic vibrational OH frequency shift, $\Delta\omega_h$(OH) (cm^{-1}); intermolecular bond distance, r(H···N)(angstroms). [b] Geometries optimized at aug-cc-pVDZ. [c] Geometries optimized at SCF/DZP level. Reference 4. [d] From a set of isotherms at different temperatures. Reference 43. [e] Microcalorimetric measurements at 300 K. Higher values in the limit of zero coverage; lower values for higher coverages. Reference 44. [f] IR spectroscopy at 4 K. Reference 39.

TABLE 4: SIL/H_2O System. See Table 3 for Description

	BE (BSSE)	$\Delta H°(0)$	ΔI(OH)	$\Delta\omega_h$(OH)	r(H···O)
present work					
B3-LYP/DZP	−35.1 (4.4)	−22.3	11	−295	1.800
B3-LYP/6-31+G(d,p)	−29.2 (4.1)	−16.6	9	−237	1.857
B3-LYP/aug-cc-pVDZ	−23.1 (1.4)	−14.2	9	−222	1.884
B3-LYP/aug-cc-pVTZ[a]	−23.4 (0.4)	−15.5			
MP2/DZP	−33.6 (6.1)	−19.1	7	−228	1.846
MP2/6-31+G(d,p)	−32.2 (8.6)	−15.2	8	−189	1.875
MP2/aug-cc-pVDZ	−26.8 (4.6)	−14.8	7	−202	1.876
MP2/aug-cc-pVTZ[a]	−27.3(2.6)	−17.3			
previous work					
SCF/DZP[b]	−25.8 (1.5)			−134	1.966
SCF/TZ+(2d,2p)[b]	−20.2				
MP2/TZ+(2d,2p)[b]	−26.1				
experimental		−25[c]		−300[f]	
		−15/−45[d]			
		−25[e]			

[a] Geometries optimized at aug-cc-pVDZ. [b] Geometries optimized at SCF/DZP level. Reference 5. [c] By a heat of immersion technique. Reference 47. [d] Microcalorimetric measurements at 300 K. Higher values in the limit of zero coverage; lower values for higher coverages. References 44 and 48. [e] Isosteric heat on silicalite. Reference 49. [f] Reference 45.

TABLE 5: SIL/CO System. See Table 3 for Description. CO Frequency Shift, $\Delta\omega_h$(CO) (cm^{-1})

	BE (BSSE)	$\Delta H°(0)$	ΔI(OH)	$\Delta\omega_h$(OH)	$\Delta\omega_h$(CO)	r(H···C)
present work						
B3-LYP/DZP	−15.1 (5.3)	−5.7	5	−83	27	2.210
B3-LYP/6-31+G(d,p)	−9.1 (1.7)	−3.6	3	−70	23	2.296
B3-LYP/aug-cc-pVDZ	−8.0 (1.5)	−2.8	4	−65	19	2.298
B3-LYP/aug-cc-pVTZ[a]	−8.2 (0.7)	−3.8				
MP2/DZP	−14.7 (5.6)	−5.3	2.8	−52	20	2.292
MP2/6-31+G(d,p)	−11.3 (3.5)	−4.2	2.6	−48	16	2.333
MP2/aug-cc-pVDZ	−12.2 (3.9)	−4.6	3.2	−59	16	2.278
MP2/aug-cc-pVTZ[a]	−12.8 (2.6)	−6.6				
previous work						
SCF/DZP[b]	−8.2 (2.7)	−1.9		−25	23	2.491
B3-LYP/6-31G(d,p)[c]	−14.3 (6.4)	−4.4		−69	27	2.238
experimental		−11.0[d]		−92[d]	15[d]	
				−78[e]	14[e]	

[a] Geometries optimized at aug-cc-pVDZ. [b] Reference 11 [c] Reference 12 [d] Reference 50 [e] Reference 51

As to the relationship between energy of interaction and shift in frequency, two possibilities are envisaged in the literature. Experimental studies in solution seem to show a linear dependence of the energy of interaction on $\Delta\omega_h$(OH), the so-called Badger−Bauer rule.[2] On the other hand, experimental data on the H-bonding of molecules onto SiOH groups in silicas indicate a linear relationship between the energy of interaction and the square root of $\Delta\omega_h$(OH), in agreement with old descriptions of H-bonding by Mulliken.[1] From the data in Tables 3−7, it is inferred that all basis sets adopted yield a linear correlation between BE(CPC) values and $[\Delta\omega_h(\mathrm{OH})/\omega_h(\mathrm{OH})]^{1/2}$ (Figure 6), in both MP2 and B3-LYP treatments (upper and lower sections of the figure, respectively), when the family of SIL are considered. However, B3-LYP data for the case BRO/CO do not align with the others, even though the shifts in frequency have been normalized to the unperturbed frequencies of SIL and BRO. The slope of the two straight lines in the MP2 and B3-LYP cases are rather close to each other. Note

TABLE 6: BRO/CO System[a]

	BE (BSSE)	$\Delta H°(0)$	ΔI(OH)	$\Delta\omega_h$(OH)	$\Delta\omega_h$(CO)	r(H···C)
present work						
B3-LYP/DZP	−24.7 (6.1)	−13.9	4.9	−229	46	2.041
B3-LYP/6-31+G(d,p)	−16.7 (2.4)	−9.8	4.4	−190	39	2.102
B3-LYP/aug-cc-pVDZ	−15.3 (2.0)	−8.5	4.9	−184	35	2.108
MP2/DZP	−24.9 (6.0)	−14.4	3.7	−174	33	2.087
MP2/6-31+G(d,p)	−20.9 (5.5)	−10.9		−141[c]		2.130
MP2/aug-cc-pVDZ[b]	−21.7 (5.4)	−11.8				
previous work						
SCF/DZP[d]	−14.5 (3.0)	−7.2		−84	38	2.304
B3-LYP/6-31G(d,p)[e]	−24.4 (8.5)	−11.0		−227	44	2.018
experimental		−13.6/−17.2[f]		−275/−340[g]	32/36[g]	2.1 ± 0.1[h]

[a] Interaction energies, BE (kJ/mol); relative change in infrared intensity of the harmonic stretching mode for the bridged hydroxyl group $\Delta I(\mathrm{OH})=(I_c - I_0)/I_0$; OH and CO frequency shifts, $\Delta\omega_h$(OH) and $\Delta\omega_h$(CO) (cm^{-1}). [b] Geometries optimized at 6-31+G(d,p). [c] Numerical differentiation. [d] Reference 11. [e] Reference 12. [f] Reference 52. [g] From different types of zeolites. Reference 11. [h] From ^{13}C-NMR spectroscopy in H−Y zeolites at 4.5 K. Reference 38.

TABLE 7: SIL/H_2 System[a]

	BE (BSSE)	$\Delta H°(0)$	ΔI(OH)	$\Delta\omega_h$(OH)	$\Delta\omega_h$(H−H)	r(H···H−H)
T-shaped						
B3-LYP/aug-cc-pVDZ	−2.89 (1.27)	2.92	1.34	−19	−11	2.137
B3-LYP/aug-cc-pVTZ[b]	−1.74 (0.19)	3.00				
MP2/aug-cc-pVDZ	−3.87 (1.74)	2.31	0.90	−7	−20	2.194
MP2/aug-cc-pVTZ[b]	−3.67 (0.80)	1.57				
	BE (BSSE)	$\Delta H°(0)$	ΔI(OH)	$\Delta\omega_h$(OH)	$\Delta\omega_h$(H−H)	r(H···H−H)
F-shaped						
B3-LYP/aug-cc-pVDZ	−1.68 (0.66)	3.27	−0.003	−1	−25	2.727
B3-LYP/aug-cc-pVTZ[b]	−1.15 (0.17)	3.31				
MP2/aug-cc-pVDZ	−3.46 (1.41)	2.70	−0.004	−3	−31	2.643
MP2/aug-cc-pVTZ[b]	−3.05 (0.70)	2.40				
experimental				−6[c]	−33[c]	

[a] Interaction energies, BE (kJ/mol); relative change in infrared intensity of the harmonic O−H stretching mode $\Delta I(\mathrm{OH})=(I_c - I_0)/I_0$; harmonic vibrational OH frequency shift, $\Delta\omega_h$(OH) (cm^{-1}); harmonic vibrational H−H frequency shift, $\Delta\omega_h$(H−H) (cm^{-1}); r, intermolecular bond distance (angstroms). [b] Geometries optimized at aug-cc-pVDZ. [c] Reference 7.

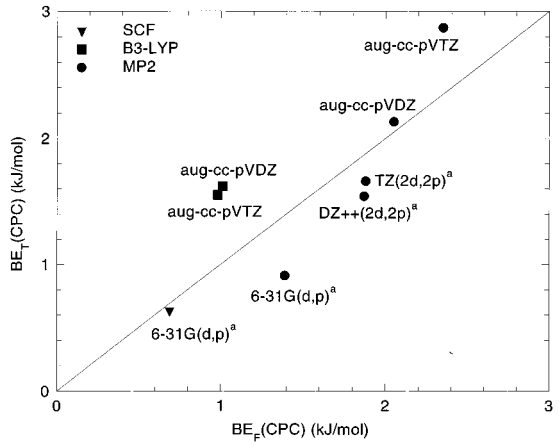

Figure 5. BE (kJ/mol) (BSSE corrected) for the T-shaped SIL/H_2 adduct versus the corresponding value for the F-shaped adduct. Data with footnote "a" are from ref 7.

that $\Delta H°(0)$ values do not correlate as neatly as BE(CPC) (figure not reported). Note as well that the straight lines in Figure 6 do not pass through the origin. We have already found a linear correlation between BE and $\sqrt{\Delta\omega_h(\mathrm{OH})}$ for a family of adducts of HF, with the same molecules considered here,[19] and of SIL and BRO with a family of unsaturated hydrocarbons.[15] A linear plot not passing through the origin, like in the present case, was observed for the adducts of HF:[19] a null intercept (i.e., a satisfactory proportionality) was instead observed in the case of adducts of SIL and BRO with a family of unsaturated hydrocarbons.[15] A possible explanation for this consists of the role of basis set superposition error. This is indeed taken into

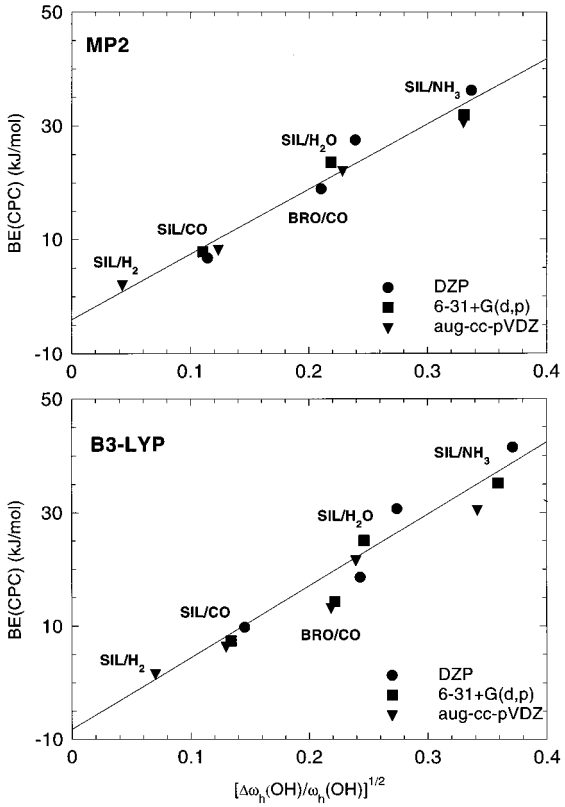

Figure 6. Correlation between BE (kJ/mol) (BSSE corrected) and $(\Delta\omega_h(\mathrm{OH})/\omega_h(\mathrm{OH}))^{1/2}$ for all adducts. Upper section, MP2 results; lower section, B3-LYP results.

TABLE 8: Anharmonicity of the OH Stretching Mode for SIL and SIL/NH_3 by Different Methods[a]

	SIL				SIL/NH_3			
	ω_{01}	ω_e	ω_h	$\omega_e x_e$	$\Delta\omega_{01}$	$\Delta\omega_e$	$\Delta\omega_h$	$\Delta\omega_e x_e$
present work								
B3-LYP/DZP	3752	3911	3919	79.8	−677	−522	−541	77.2
B3-LYP/6-31+G(d,p)	3739	3895	3903	78.1	−639	−477	−504	80.8
B3-LYP/aug-cc-pVDZ	3705	3861	3867	78.1	−571	−429	−452	71.1
MP2/DZP	3814	3975	3983	80.4	−577	−427	−452	75.1
MP2/6-31+G(d,p)	3789	3946	3953	78.5	−562	−403	−432	79.5
MP2/aug-cc-pVDZ	3708	3863	3870	77.4	−549	−400	−422	74.4
previous work								
SCF/DZP	4090	4246	4250	78.0				
B3-LYP/6-31G(d,p)[b]	3730	3890		80.0				
experimental	3748[c]	3919[c]						
	3744[d]	3941[d]		98[d]	−950[e]			

[a] ω_{01}, fundamental, and ω_{02}, first overtone, frequencies; ω_e, harmonic frequency; $\omega_e x_e$, anharmonicity parameter; and ω_h, fully coupled harmonic frequency. Units are in cm^{-1}. [b] Reference 12. [c] Reference 7. [d] Reference 51. [e] IR spectroscopy at 4 K. Reference 39.

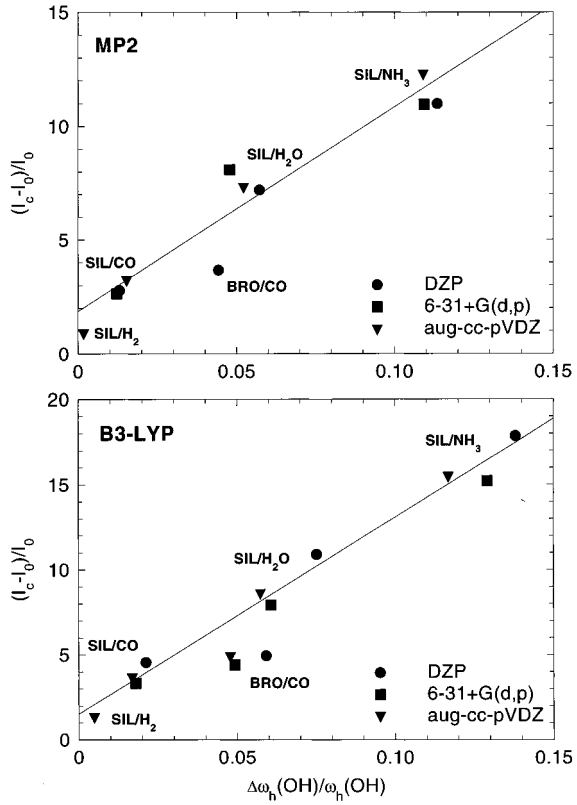

Figure 7. Correlation between $\Delta I(OH) = (I_c - I_0)/I_0$ and $\Delta\omega_h(OH)/\omega_h(OH)$ for all adducts. Upper section, MP2 results; lower section, B3-LYP results.

account in the case of BE in some way: no similar correction is however done for other observables such as the shift in frequency, which is also bound to be affected by BSSE. Most probably, inaccuracies introduced by BSSE play a more marked role in a set of different molecules than in the case of similar hydrocarbons, in which smaller binding energies were, however, computed.

Figure 7 reports the relative change in the intensity of the OH stretch mode ($\Delta I(OH) = (I_C - I_0)/I_0$) in the various cases as a function of the relative shift $\Delta\omega_h(OH)/\omega_h(OH)$. Data concerning SIL adducts, irrespective of the level of treatment, nicely line up on the same straight line. Data concerning BRO/CO fall outside the straight line: we have indications from similar results concerning HF adducts[19] that further data concerning BRO adducts would probably line up on a straight line with a smaller slope. The straight line does not pass, however, through the origin: the possible explanation is the same advanced above (i.e., the role of BSSE on observables other than the interaction energy).

3.6. Anharmonicity of the O−H Motion. It is well-known that, when a proton is involved in a vibration, a relatively large deviation from the harmonic approximation is to be expected. Indeed, the measurement of a family of overtones for both SiOH and Si(OH)Al has enabled Kazansky and co-workers, as quoted above, to estimate both the harmonic frequency ω_h and the anharmonicity parameter $\omega_e x_e$ in both cases. These are reported in Table 8, together with our estimates for SIL according to various levels of treatment. It is observed that the values for the anharmonicity parameter are in excellent agreement as far as SIL is concerned: as it concerns SiOH/NH_3, absorptions other than the fundamental were not observed, and this fact was interpreted as evidence that the second vibrational excited level is above the energy barrier for the dissociation of the complex.[31] A substantial increase in anharmonicity is indeed obtained as a result of calculations, and in conclusion the transition ω_{01} is much larger than ω_e for the adduct SIL/NH_3. As already pointed out above, B3-LYP values for $\Delta\omega_{01}$ are much more basis set dependent that the corresponding MP2 values: unscaled values for either ω_h or ω_{01} show instead an opposite basis set dependence.

3.7. Comparison with Experiment: Relative Acidity of the Cluster Models and the Actual Surface Structures. When comparing experimental results and computational ones concerning H-bonded systems, some caution must be in general exercised, and the present cases are no exception. As far as $\Delta H°(0)$ is concerned, direct calorimetric data are only available for room temperature measurements, since adsorption calorimetry at low temperature is a rather difficult technique. Energetic data for the interaction of CO with isolated hydroxyls of silica or Brønsted sites in zeolites come from much less accurate determination of isosteric heats.

As far as $\Delta\omega_h(OH)$ is concerned, it has to be pointed out that it is not possible to measure the shift imparted by a single water molecule to the stretching mode of a single isolated hydroxyl of amorphous silica, because simultaneously aggregates of water molecules are formed, so that the IR signal due to the SiOH species engaged in H-bonding is buried by the signals arising from the water molecules. There are indications, however, that $\Delta\omega_h(OH)$ must be in the neighborhood of 300 cm^{-1}.[5,45] Recent work[46] has also highlighted the relevance of multiple interactions between the adsorbed water proton and the nearby siloxane bridge.

In the case of ammonia interacting with the isolated hydroxyl of silica, IR measurements carried out at room-temperature yield

$\Delta\omega_h(OH) = -650$ cm^{-1}. Bands due to H-bonded hydroxyls are known to shift to lower frequency when decreasing the temperature: Tziganenko has measured a value of -950 cm^{-1} at 4 K.[39] Since the computational results are estimated at absolute zero, this latter is the reference value to be compared with. Such effect is likely to be less important in the presence of weak interactions such as those of CO, which are already measured at low temperature (77 K).

The $\Delta\omega_h(OH)$ value in the case of SIL/NH_3 affords a reliable comparison between experiment and theory, because, on one hand, a firm reference value is at hand. On the other hand, calculations using two different procedures (MP2 and B3-LYP) have yielded with the best basis set used similar results, both as far as the interaction energy and the shift in the harmonic frequency are concerned. Moreover, the anharmonic frequencies of SIL/NH_3 calculated both at MP2 level and by the B3-LYP method are in close agreement. Such values may thus be considered as reliable, and therefore one can assign with some confidence the value of -570 ± 30 cm^{-1} to the adduct SIL/NH_3. The evident difference from the value of -950 cm^{-1} must therefore be ascribed to a difference in intrinsic acidity between SIL and the actual SiOH group at the surface of silica.

4. Conclusions

The comparison between the various levels of calculations confirms what is an emerging trend in the literature (i.e., the efficiency of nonlocal density functional methods): indeed, the comparison with MP2 shows that similar results are obtained as far as all important observables are concerned. It has to be stressed, however, that B3-LYP (as well as probably other gradient-corrected methods) shows a significative basis set dependence, in particular for the calculation of vibrational shifts. Standard basis sets such as the 6-31G(d,p) will give frequency shifts and binding energies which are too large. On the other hand, the widespread procedure of computing the binding energy with large basis sets at the geometry optimized with much smaller basis sets holds also for the B3-LYP method. Indeed the ΔE computed at aug-cc-pVTZ//DZP for the SIL/NH_3 adduct (BE = 32.5 kJ/mol^{-1}, BSSE = 0.6 kJ/mol^{-1}) is indistinguishable from our best estimate.

The availability of a set of data concerning interactions of different strength allows some correlations to be drawn, as customarily done with experimental data about H-bonds. The increasing shift of the OH stretching mode, as well as its intensification, with increasing strength, are well accounted for by B3-LYP: indeed, the correlations observed are quite close to those resulting for MP2. Finally, the case for SIL/NH_3 has been studied in greatest detail, by using the highest basis set and studying the anharmonicity of the OH motion. MP2 and B3-LYP methods give similar results, so that it can be assumed that the zero-temperature value of $\Delta\nu_{01}$ does not exceed 600 cm^{-1}. The experimental value of 950 cm^{-1}, together with other evidence listed above, strongly suggests the weaker acidic nature of SIL with respect to SiOH. This fact is probably the reason why calculations yield ambiguous and unsatisfactory results for the SIL/H_2 adduct.

References and Notes

(1) Sauer, J.; Ugliengo, P.; Garrone, E.; Saunders: V. R. *Chem. Rev.* **1994**, *94*, 2095.

(2) Pimentel, G. C.; McLellanm A. L. *The Hydrogen Bond*; Freeman: San Francisco, 1960.

(3) Sauer, J.; Ahlrichs, R. *J. Chem. Phys.* **1990**, *93*, 2575.

(4) Ugliengo, P.; Saunders: V. R.; Garrone, E. *Surf. Science* **1988**, *224*, 498.

(5) Ugliengo, P.; Saunders: V. R.; Garrone, E. *J. Phys. Chem.* **1990**, *94*, 2260.

(6) Ugliengo, P.; Saunders: V. R.; Garrone, E. *Chem. Phys. Lett.* **1990**, *169*, 501.

(7) Garrone, E.; Kazansky, V. B.; Kustov, L. M.; Sauer, J.; Senchenya, I. N.; Ugliengo, P. *J. Phys. Chem.* **1992**, *96*, 1040.

(8) De Almedia, W. B.; O'Malley, P. J. *J. Chem. Soc., Chem. Commun.* **1991**, *7*, 455.

(9) Ugliengo, P.; Saunders: V. R.; Garrone, E. *J. Phys. Chem.* **1989**, *93*, 5210.

(10) Bates, S.; Dwyer, J. *J. Phys. Chem.* **1993**, *97*, 5897.

(11) Senchenya, I. N.; Garrone, E.; Ugliengo, P. *J. Mol. Struct. (THEOCHEM)* **1996**, *368*, 93.

(12) Farnworth, K. J.; O'Malley, P. J. *J. Phys. Chem.* **1996**, *100*, 1814.

(13) Garrone, E.; Ugliengo, P.; Ghiotti, G.; Borello, E.; Saunders: V. R. *Spectrochim. Acta* **1993**, *A49*, 1221.

(14) Nicholas, J. B.; Winaus, R. E.; Harrison, R. J.; Iton, L. E.; Curtiss, L. A.; Hopfinger, A. J. *J. Phys. Chem.* **1992**, *96*, 10247.

(15) Ugliengo, P.; Ferrari, A. M.; Zecchina, A.; Garrone, E. *J. Phys. Chem.* **1996**, *100*, 3632.

(16) Møller, C.; Plesset, M. S. *Phys. Rev.* **1934**, *46*, 618.

(17) Parr, R. G.; Yang, W. *Density Functional Theory of Atoms and Molecules*; Oxford University Press: Oxford, 1989.

(18) Novoa, J. J.; Sosa, C. *J. Phys. Chem.* **1995**, *99*, 15837. Topol, I. A.; Burt, S. K.; Rashin, A. A. *Chem. Phys. Lett.* **1995**, *247*, 112. Hobza, P.; Sponer, J.; Reschel, T. J. *J. Comput. Chem.* **1995**, *16*, 1315. Kieninger, M.; Suhai, S. *Int. J. Quantum Chem.* **1994**, *52*, 465. Jeanvoine, Y.; Bohr, F.; Ruiz-Lopez, M. F. *Can. J. Chem.* **1995**, *73*, 710. Del Bene, J.; Person, W. B.; Szczepaniak, K. *J. Phys. Chem.* **1995**, *99*, 10705. Kim, K.; Jordan, K. D. *J. Phys. Chem.* **1994**, *98*, 10089.

(19) Civalleri, B.; Ugliengo, P.; Garrone, E. *J. Mol. Struct. (THEOCHEM)* **1997**, *419*, 227. Ugliengo, P.; Civalleri, B.; Garrone, E. *Nuovo Cimento D* **1997**, *19*, 1765.

(20) Frisch, M. J.; Trucks, G. W.; Schlegel, H. B.; Gill, P. M. W.; Johnson, B. G.; Robb, M. A.; Cheeseman, J. R.; Keith, T. A.; Petersson, G. A.; Montgomery, J. A.; Raghavachari, K.; Al-Laham, M. A.; Zakrzewski, V. G.; Ortiz, J. V.; Foresman, J. B.; Cioslowski, J.; Stefanov, B. B.; Nanayakkara, A.; Challacombe, M.; Peng, C. Y.; Ayala, P. Y.; Chen, W.; Wong, M. W.; Andres, J. L.; Replogle, E. S.; Gomperts, R.; Martin, R. L.; Fox, D. J.; Binkley, J. S.; Defrees, D. J.; Baker, J.; Stewart, J. P.; Head-Gordon, M.; Gonzalez, C.; Pople, J. A. Gaussian 94, Revision C.3; Gaussian, Inc.: Pittsburgh, PA, 1995.

(21) Becke, A. D. *J. Chem. Phys.* **1993**, *98*, 5648.

(22) Lee, C.; Yang, W.; Parr, R. G. *Phys. Rev.* **1988**, *B37*, 785.

(23) Dunning, T. H., Jr.; Hay, P. J. *Methods of Electronic Structure Theory*; Schaefer, H. F., III, Ed. (Mod. Theor. Chem.) Vol. 3: Pleomegam, 1977; pp 1−27. Huzinaga, S. *J. Chem. Phys.* **1965**, *42*, 618. Huzinaga, S. *Approximate Atomic Wave functions. II*; Department of Chemistry Report; University of Alberta: Edmonton, Alberta, 1971. Dunning, T. H., Jr. *J. Chem. Phys.* **1989**, *90*, 1007.

(24) Hehre, W. J.; Radom, L.; Schleyer, P.v.R.; Pople, J. A. *Ab Initio Molecular Orbital Theory*; Wiley: New York, 1986.

(25) Kendall, R. A.; Dunning, T. H., Jr.; Harrison, R. J. *J. Chem. Phys.* **1992**, *96*, 6796. Woon, D. E.; Dunning, T. H., Jr. *J. Chem. Phys.* **1993**, *98*, 1358. Woon, D. E.; Dunning, T. H., Jr. *J. Chem. Phys.* **1994**, *100*, 2975.

(26) Boys, S. F.; Bernardi, F. *Mol. Phys.* **1970**, *19*, 553.

(27) Wilson, E. B.; Decius, J. S.; Cross, P. C. *Molecular Vibrations*; McGraw-Hill: New York, 1955.

(28) Ugliengo, P. ANHARM; 1989. Unpublished. (A program to solve monodimensional Schrödinger equation.)

(29) Nicholas, J. B.; Feyereisen, M. *J. Chem. Phys.* **1995**, *103*, 8031.

(30) Damrauer, R.; Simon, R.; Krempp, M. *J. Am. Chem. Soc.* **1991**, *113*, 4432.

(31) Kazansky, V. B.; Gritskov, A. M.; Andreev, V. M.; Zhidomirov, G. M. *J. Mol. Catal.* **1978**, *4*, 135.

(32) Dobbs, K. D.; Dixon, D. A. *J. Phys. Chem.* **1994**, *98*, 4498.

(33) Paukshtis, E. A.; Yurchenko, E. N. *Usp. Khim.* **1983**, *52*, 436.

(34) Zygmunt, S. A.; Brand, H. V.; Lucas, D. J.; Iton, L. E.; Curtiss, L. A. *J. Mol. Struct. (THEOCHEM)* **1994**, *314*, 113.

(35) Makarova, M. A.; Ojo, A. F.; Karim, K.; Hunger, M.; Dwyer, J. *J. Phys. Chem.* **1994**, *98*, 3619.

(36) Brunner, E.; Pfeifer, H. *Z. Phys. Chem.* **1995**, *192*, 77.

(37) Freude, D.; Klinowski, J.; Hamdan, H. *Chem. Phys. Lett.* **1988**, *149*, 355.

(38) Koch, M.; Brunner, E.; Pfeifer, H.; Zscherpel, D. *Chem. Phys. Lett.* **1994**, *228*, 501.

(39) Tsiganenko, A. A.; Babaeva, M. A. *Opt. Spectrosc.* **1983**, *54*, 665.
(40) Mastikhin, V. M.; Mudrakovsky, I. L.; Nosov, A. V. *Bruker Rep.* **1989**, *2*, 18.
(41) Datka, J.; Boczar, M.; Rymarowicz, P. *J. Catal.* **1988**, *114*, 368.
(42) Datka, J.; Boczar, M.; Gil, B. *Langmuir* **1993**, *9*, 2496.
(43) Hertl, W.; Hair, M. L. *Nature* **1969**, *223*, 1950.
(44) Fubini, B.; Bolis, V.; Cavenago, A.; Garrone, E.; Ugliengo, P. *Langmuir* **1993**, *9*, 2712. Fubini, B.; Bolis, V.; Cavenago, A.; Ugliengo, P. *J. Chem. Soc., Faraday Trans.* **1992**, *88*, 277.
(45) Zecchina, A.; Geobaldo, F.; Spoto, G.; Bordiga, S.; Ricchiardi, G.; Buzzoni, R.; Petrini, G. *J. Phys. Chem.* **1996**, *100*, 16584.
(46) Pelmenschikov, A. G.; Morosi, G.; Gamba, A. *J. Phys. Chem. A* **1997**, *101*, 1178.
(47) Bassett, D. R.; Boucher, E. A.; Zettlemayer, A. C. *J. Coll. Interface Sci.* **1970**, *34*, 3.
(48) Bolis, V.; Fubini, B.; Marchese, L.; Martra, G.; Costa, G. *J. Chem. Soc., Faraday Trans.* **1991**, *87*, 497. Fubini, B.; Bolis, V.; Bailes, M.; Stone, F. S. *Solid State Ionics* **1989**, *32/33*, 258. Bolis, V.; Marchese, L.; Coluccia, S.; Fubini, B. *Adsorp. Sci. Technol.* **1988**, *5*, 239.
(49) Flanigen, E. M.; Bennett, J. M.; Grose, R. W.; Cohen, J. P.; Patton, R. L.; Kirchner, R. M.; Smith, J. V. *Nature* **1978**, *271*, 512.
(50) Echoufi, N.; Gelin, P. *J. Chem. Soc. Trans.* **1992**, *88*, 1067.
(51) Ghiotti, G.; Garrone, E.; Morterra, C.; Zecchina, A. *J. Phys. Chem.* **1979**, *83*, 2863.
(52) Gupta, N. M.; Kamble, V. S.; Rao, K. A.; Iyer, R. M. *J. Catal.* **1989**, *120*, 432.